WAVE PROPAGATION IN FLUID-FILLED PIPES

F.J. FAHY & C.R. FULLER

I.S.V.R. UNIVERSITY OF SOUTHAMPTON

Introduction

Wave propagation in a fluid-filled pipe involves coupled motions of the solid and fluid components. It is not in principle possible separately to identify "structural" waves, or "fluid" waves, although, under some circumstances, the energy in one of the components may far outweigh that in the other; axial wavenumbers, and phase and group velocities must necessarily be identical in both media. A free wave in a pipe is characterised by its axial wavenumber-frequency, or dispersion curve, and its circumferential mode order. In a thin-walled pipe in-vacuo each circumferential mode order is associated with three different dispersion curves, or branches. At any particular frequency the wave motion corresponding to each branch involves different ratios of the radial, axial and tangential displacements. The ratios associated with each branch vary with frequency, thereby rendering the commonly encountered terms "flexural wave", "longitudinal wave" and "torsional wave" somewhat misleading. The pressure of fluid within the shell increases the number of branches greatly which further complicates the labelling and physical interpretation of the branches.

A further complication of wave behaviour in undamped cylindrical shells, both in-vacuo and fluid-filled, is the existence of waves of complex wavenumber. This phenomenon is not only puzzling from a physical point of view, but makes the task of computing the wavenumbers, and tracing each branch, lengthy and difficult. However, because one of the major applications of the results of free wave analysis is the generation of impedance characteristics for use in the investigation of the effects of applied forces and moments, and of discontinuities in pipework, on noise and vibration radiation and transmission, all possible free wave branches must be identified and included. This paper summarises the results of free wave analysis of thin-walled, fluid-filled pipes and presents a discussion of dispersion curve characteristics, and ratios of propagating energy flux, in the two media. The purpose is primarily to attach physical significance to the results and not to argue analytical details.

Dispersion Analysis

Kumar (1) and Merkulov (2) have previously presented the most general analyses of this problem of free wave propagation in fluid-filled elastic shells, while numerous other authors have presented analyses involving various approximations, thereby restricting the usefulness of their results. Kumar deals only with axi-symmetric modes of fairly thick-walled shells, and provides little physical interpretation of his results, while Merkulov omits the complex branches.

The Donnell-Mushtari shell equations are employed in the present analysis; the effects of rotary inertia and transverse shear are omitted. The fluid is assumed to be inviscid and perfectly elastic. The circumferential variations of the fields are assumed to be of the form cos/sin$(n\theta)$, the frequency is ω and the axial wavenumber k_{ns}, where the subscript s denotes a particular dispersion branch. The acoustic pressure field takes the form

$$p = \sum_{s=0}^{\infty} \sum_{n=0}^{\infty} P_{ns} \cos(n\theta) J_n(k_s^r r) \exp i(\omega t - k_{ns} x).$$

Substitution into the radial force shell equation yields a matrix equation in terms of the coefficients of axial motion U_{ns}, tangential motion V_{ns}, and radial motion W_{ns}, of the shell and the pressure coefficients P_{ns}. The condition of continuity of radial velocity at the shell wall allows P_{ns} to be written in terms of W_{ns}. The 3 x 3 matrix terms contain squares of the non-dimensional frequency parameter $\Omega = \omega a/c_L$, and of the shell thickness parameter $\beta = h^2/12a^2$, powers of $(k_{ns}a)$ and of n of up to 4, and a fluid loading term $FL = \Omega^2(\rho_f/\rho_s)(h/a)^{-1}(k_s^r a)^{-1}\left[J_n(k_s^r a)/J_n'(k_s^r a)\right]$.

Equation of the determinant of the matrix equation to zero yields the characteristic dispersion equation. The roots of this equation were found by using a complex root searching technique on an ICL 2900 computer. Initial values were chosen to be those of the in-vacuo bending near field (3). Dispersion curves were obtained for shells of steel and hard rubber, filled with water, with $n = 0$ and 1 and wall thickness ratios $h/a = 0.05$ and $h/a = 0.005$. An example is shown in Figure 1 in which $n = 0$, $h/a = 0.05$ and the material is steel.

The branches having real wavenumbers are discussed first. Two branches exist at low frequencies. The $s = 1$ branch is close to that of a plane fluid wave in a rigid-walled tube. The $s = 2$ branch is close to the in-vacuo "flexural" shell branch which is largely extensional in nature. As Ω is increased the coupling of shell and fluid motion increases; $s = 2$ approaches the first pressure release duct mode and $s = 1$ approaches the in-vacuo flexural mode. The branch $s = 3$ cuts on at $\Omega = 0.85$. It initially follows the corresponding extensional in-vacuo shell branch (which cuts on at $\Omega = 1.0$) until $\Omega \gtrsim 1.3$, when it turns sharply to approach the second rigid-walled duct mode. Near this frequency $s = 4$ cuts on as a fluid wave in a duct with compliant walls and then turns into a plateau where it behaves like an extensional in-vacuo shell wave until finally reverting to a fluid like wave for $\Omega > 2.3$. Higher s branches cut on as "fluid" waves, at frequencies close to the rigid-wall duct cut-off frequencies, change to follow the in-vacuo extensional wave branch as "shell" waves, and then revert to fluid-like waves at a frequency where the in-vacuo shell branch crosses the rigid-walled duct branch. These "conversion" regions correspond to intersections of the dispersion curves for the uncoupled solid and fluid waveguides, i.e., a form of coincidence.

In the purely imaginary plane the branches at low frequencies correspond to the rigid-walled duct modes below cut-off; this is due to the rigidity of the shell at low frequencies. As the frequency increases the shell becomes less stiff in the radial direction and the branches fall between the rigid-walled and pressure release solutions. Finally the imaginary branches terminate at the $k_{ns} = 0$ axis (cut-off) whence they proceed as real branches. At low values of Ω the complex branches correspond closely to those for an in-vacuo shell. The real parts of the $s = 4$ and $s = 6$ branches are of opposite sign; the imaginary parts have equal value to the former, but are of the same sign. These complex waves must exist simultaneously and have equal amplitudes, so that the energy conservation principle is not violated. The associated radial pressure variation in the fluid takes the form of an evanescent interference pattern. At higher frequencies the complex branches form branch links which leave the imaginary plane (with opposite signs of the real parts) at the peak of a "meander" and re-enter the imaginary plane at the rear of the next meander (e.g. (5,6), (7,6), (8,6) in Figure 1). The paired complex branches, for example s = 7 and 6, would, by analogy with real valued branches, appear to exhibit near-field coincidence behaviour.

The primary effect of reducing the shell thickness by a factor of 10 is to move the fluid-like branches towards pressure release duct mode behaviour. The s = 2 branch remains largely unchanged because the low frequency "flexural" wave in the shell is largely extensional in nature, and it behaves like a pressure release mode at high frequencies. The s = 1 branch changes radically, swinging upwards and tending to ∞ at $\Omega \to 1.0$; it ultimately disappears completely as $h/a \to 0$. It has very low group and phase velocities over most of the frequency range. Similarly, the complex branches disappear as $h/a \to 0$. The imaginary branches remain like rigid-walled duct modes at very low frequencies but move towards pressure-release behaviour with increasing Ω; they cut-on as nearly pressure-release modes, transform into the extensional shell branch and then veer away again to asymptote to pressure release behaviour. The complex branches do not intersect the imaginary plane and therefore near field coincidence behaviour does not occur in very thin shells.

With a hard rubber shell, in which the sound speed is much less than in steel ($\approx$ 3.7:1), the acoustic modes do not cut-on until much higher values of Ω. Because it does not intersect any fluid branches the s = 2 branch behaves as a shell wave over the whole frequency range considered ($0 < \Omega < 4.0$): the plateau behaviour observed in steel shells is generally absent. The s = 1 branch approximates to a plane acoustic wave at very low frequencies, but quickly changes to that of an acoustically slow "shell" wave, rather like that in the very thin-walled steel shell. The high fluid impedance at frequencies below the duct cut-off frequencies prevents the n = 0 extensional shell wave from cutting-on at $\Omega = 1.0$, as it would in-vacuo. At $\Omega = 2.48$ the s = 3 branch cuts-on as an acoustic mode in a slightly compliant tube, and then rapidly asymptotes to a pressure-release mode.

Energy Distributions

The ratio of energy flux in the fluid to that in the shell can be shown to be given by $E_r = \Omega^2(\rho_f/\rho_s)(k^r_{ns}a)(k^r_s a\, J_n'(k^r_s a))^{-2}(F_f/S_f)$, where F_f and S_f are given at the end of the paper. This ratio is plotted for a water-filled steel shell of h/a = 0.05, and n = 0, in Figure 2. At low frequencies the energy travels primarily either in the fluid (s = 1) or in the solid (s = 2). At $\Omega \approx 0.82$ the ratio in both branches is unity; above this frequency the distributions reverse. Just above the cut-off frequencies of the higher modes, in the plateau region, (s > 3) the energy resides primarily in the solid; as the branch moves towards a more fluid-like wave behaviour, the energy moves strongly into the fluid medium. This type of behaviour is exhibited by all higher modes. In general, then the energy ratio is either much greater than or much less than unity in the n = 0 modes. In the n = 1 modes this is not so clearly the case, although values of E_r close to unity are relatively rare.

Conclusion

Approximate models of fluid-filled shells, especially those neglecting axial shell motion, are likely to product highly misleading results. Propagation modes tend to be either shell or fluid dominated. The actual response, or energy fluxes in any particular case will depend upon the form of excitation.

Appendix

$$S_f = (h/a)^3/6\left[(k_{ns}a)^3 + \nu n^2(k_{ns}a) + R_a(k_{ns}a)^2 + nk_t\right] + (h/a)\left[(k_{ns}a)R_a^2 + \right.$$
$$\left. + n\nu R_a R_t + \nu R_a\right] + (h/2a)(1-\nu)(1-\nu^2)\left[nR_aR_t + (k_{ns}a)R_t^2\right]$$

where $R_t = V_{ns}/W_{ns}$ and $R_a = U_{ns}/W_{ns}$. $F_f = \frac{1}{2}\left[(J_n'(k_s^r a))^2 + (1-(n/k_s^r a)^2 J_n^2(k_s^r a)\right]$.

References

1. R. KUMAR 1972 Acustica 27, 317-329. Dispersion of axially symmetric waves in empty and fluid-filled cylindrical shells.
2. V.N. MERKULOV, V.YU. PRIKHODKO and V.V. TYUTEKIN 1978 Soviet Physics Acoustics 24(5), 405-409. Excitation and propagation of normal modes in a thin cylindrical elastic shell filled with fluid.

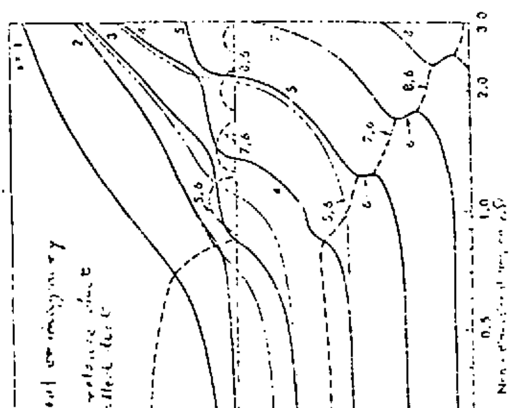

FIG.1

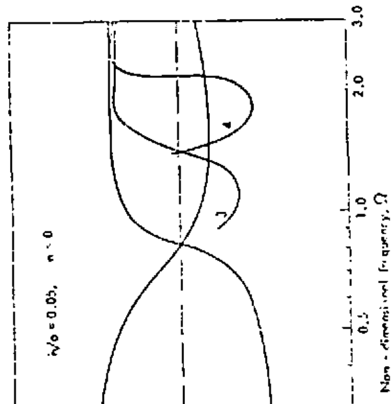

FIG.2

This research was sponsored by the Ministry of Defence.